Desalination 314 (2013) 130–138

Contents lists available at SciVerse ScienceDirect

Desalination

journal homepage: www.elsevier.com/locate/desal

Energetic performance optimization of a capacitive deionization system operating with transient cycles and brackish water

Onur N. Demirer, Rachel M. Naylor, Carlos A. Rios Perez, Ellen Wilkes, Carlos Hidrovo *

The University of Texas at Austin, 1 University Station, C2200, Austin, TX 78712, USA

HIGHLIGHTS

- Transient cycle tests are performed on a capacitive deionization cell.
- Desalination/regeneration durations are varied to find an optimum point.
- Three different criteria are used to evaluate system efficiency.
- System timing, inlet solution salinity and scale effects are investigated.

ARTICLE INFO

Article history:
Received 3 August 2012
Received in revised form 19 December 2012
Accepted 18 January 2013
Available online xxxx

Keywords:
Capacitive deionization
Performance
Energetic analysis

ABSTRACT

Water desalination using capacitive deionization (CDI) has been a recent topic of intense research as a novel technique for water desalination, capable of returning a fraction of the input energy during the regeneration of nanoporous electrodes used for ion adsorption. Usually, a set of consecutive and alternating desalination–regeneration processes is conducted to evaluate the performance of this type of systems under different operational conditions (applied electric potential, flow rate, and initial solution concentration). However, the effect of timing for desalination and regeneration processes on the performance of a capacitive deionization system has not been explored yet. This paper analyzes the effect of varying the duration of desalination and regeneration processes on overall system performance for three different salinity levels and three different CDI system sizes. More specifically, the variation in energy recovery ratio, thermodynamic efficiency, and net energy required per moles of salt adsorbed per unit of volume treated are evaluated. To optimize the timing for transient operation, one desalination test was performed until total saturation, which is identified by the outlet concentration returning to inlet concentration. From this experiment, three characteristic times were obtained: one that minimizes the outlet solution concentration, one that gives the highest adsorbed ions per energy input and one that corresponds to maximum average adsorption rate. The results obtained from testing these three timing strategies in an alternating desalination–regeneration process suggest the existence of different optimal operational points, depending on the specific needs, such as maximum desalination rate or maximum energy efficiency. The methodology presented in this paper can be extended to other operational conditions/systems to optimize their energetic performance.

1. Introduction

As the world population continues to increase, recently exceeding 7 billion [1], it is seen that providing fresh water for this increasing population with the limited natural resources is getting more and more challenging [2,3]. Water is no doubt one of the most fundamental human needs; therefore it is of very high importance. Statistics indicate that around one fifth of world population live in areas of water scarcity, and another one quarter face economic water shortage [4], meaning that effective steps have to be taken, in terms of increasing water supply or managing water demand, to overcome this problem. Since 97.5% of the water supplies are saltwater and only 0.3% of freshwater sources are readily drinkable [5], desalination is a key technology to increase both the quantity and quality of water supply. Although significant amount of desalination research has been focused on large scale desalination of high salinity water, there is a substantial potential in low cost and high efficiency desalination of brackish water to be implemented at a much smaller, local scale. Capacitive deionization (CDI) represents a viable alternative for such an application, which may be used to process the large amount of water in estuaries and underground water aquifers [6].

Desalination methods are generally grouped according to their basic principles of operation such as thermal, membrane, or electrical processes. Thermal desalination is by far the oldest method and was the first to be commercially viable [7]. The general mechanism of

* Corresponding author. Tel.: +1 512 232 0865; fax: +1 512 471 1045.
E-mail address: hidrovo@mail.utexas.edu (C. Hidrovo).

0011-9164/$ – see front matter
http://dx.doi.org/10.1016/j.desal.2013.01.014

this process is the evaporation of a solution, which results in a solid by-product and a vaporized liquid. Once this liquid is condensed, the product will be pure water. However, the high energy of vaporization for water requires that a high level of energy be input into the system [2]. Despite this drawback, multistage flash distillation is a common commercial desalination [8]. On membrane desalination, the basic theory relates back to older methods of straining liquids. Modern technologies have led to manufacturing of synthetic membranes with the ability to selectively filter certain ions in a flow [2,9]. Despite the lack of thermal energy input needed on membrane technologies, the driving pressure gradient that must be applied can become significantly large as the pore size of the membrane decreases. Generally this process is implemented as either reverse osmosis or membrane electro-dialysis [2,10]. Last, electrically based desalination methods rely upon the application of an electric potential to sustain an electric field to facilitate the movement of contaminant ions to a storage location. Two fundamentally different methods of achieving this result are capacitive deionization (CDI) and electro-dialysis [2].

Capacitive deionization is a relatively new technology that was developed as recently as the late 1960s [11,12]. While the general operating principle of the process may seem simple, an electric field pulls charged ions in the flow stream to a porous electrode to be stored, the capacity of most porous materials before this time period were limited [2,13]. With increasing developments in high surface area materials, most particularly carbon-based aerogels, veils and activated carbon electrodes, the capacity to store ions has reached a level that made CDI a process that could be practical and economically feasible [13–15]. Today, CDI is a promising desalination method since it does not utilize any chemicals, electrodes are less subject to fouling than membranes, the system is low maintenance and the operation principle dictates that it can remove any type of ionic pollutants from water.

Since the storage of ions in the pores of electrodes is the essential goal of a CDI system, these electrodes will saturate over time and the ionic concentration of the outlet solution will increase until it reaches the same concentration as that of the inlet, indicating no net ionic adsorption inside the CDI cell. At this point, it becomes necessary to clean the electrodes to restore their adsorption capacity. This process, called restoration or regeneration, can be performed by either short-circuiting the electrodes [16] or by applying an opposite voltage to the electrodes. An added benefit obtained through the regeneration process (when short-circuiting) is the return of a fraction of the energy input. This revenue of energy serves to further lower the energy requirements of the process raising its potential as a viable desalination process.

The potential that a CDI system offers can be better realized through proper calibration and operation. For any large-scale operation to be economically feasible, it would need to operate multiple CDI cells consisting of reasonably short, alternating desalination and regeneration cycles [3,17,18]. The inefficiencies caused by unoptimized timing of desalination and regeneration cycles would scale up with the system and would be detrimental to economic feasibility of the system. However, the effects of varying the timing of desalination and regeneration processes on the performance of a capacitive deionization system have not yet been examined. In this regard, publications available in the literature focus on varying other operation parameters (such as applied electric potential and solution flow rate) and lack (or not mention) an optimization criteria to select the time when a system will alternate from desalination to regeneration and vice versa [3,16–20].

This paper expands the analysis of Demirer et al. [21] to evaluate the energetic performance optimization of a CDI system at three different brackish salinity levels and three different CDI system sizes to explain the effects of timing, salinity and physical scale on CDI system performance.

2. Methodology

This section first describes the experimental set-up used for this paper. Then, we present the procedure to conduct and analyze long desalination tests, which will be called steady tests, to determine several pivotal points that will later be used to calibrate short and alternating desalination–regeneration processes, which will be called transient tests. The naming “steady” and “transient” is due to the fact that desalination is continued until total electrode saturation so that steady state is reached in the long desalination test, whereas the electrodes are never totally saturated and steady state conditions are never reached in transient tests. Last, three evaluation criteria are introduced to evaluate the performance of these alternating transient tests.

2.1. Experimental set-up

Experimental investigation about the effects of CDI process on aqueous solutions with low concentrations was conducted in the Multiscale Thermal Fluids Laboratory at The University of Texas at Austin.

Three CDI cells with flat plate electrode configuration were manufactured for fundamental modeling and energetic analyses at three different CDI system sizes. The outer casing of a CDI cell was constructed from two pieces of acrylic due to electrical insulation and both pieces were machined to form a thin inner channel with a rectangular cross-section for fluid flow. Inside the cell, two pieces of high surface area carbon aerogels obtained from Marketech Industries, measuring 25×250 mm, were placed on top and bottom faces of the flow channel and both were backed by high conductivity non-corrosive electrodes made of titanium. These carbon aerogels are specified as grade II, containing an approximate surface area of 600 $m^2\cdot g^{-1}$ and serve as the ion storage medium for our experiments. Between the two pieces of porous carbon aerogels, a polymer mesh was placed to prevent short-circuiting between anode and cathode electrodes, while still allowing proper fluid flow with minimal pressure drop through the cell. The exploded view of CDI cell assembly is presented in Fig. 1.

A schematic overview of experimental setup, similar to [22], is provided in Fig. 2. The electrical power to the control relay and CDI cell is provided by an Agilent E3647A power supply which is connected to a computer via RS-232 serial port so that it can be controlled and monitored via software. The fluid flow is driven by an Aqua Lifter AW-20 pump and the flow rate is regulated by needle valves downstream of this pump. The flow rate is monitored either

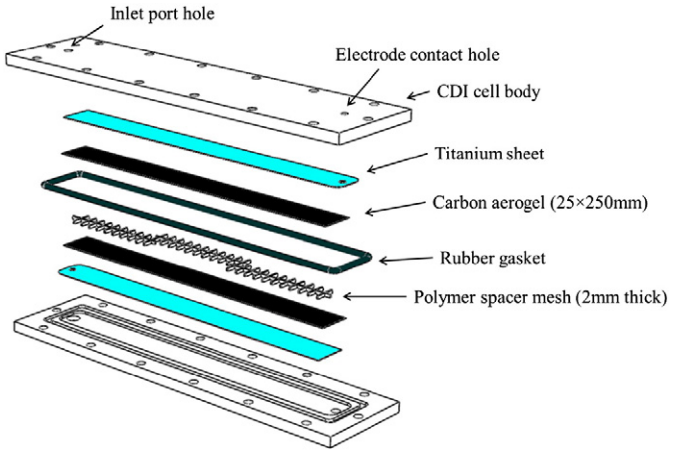

Fig. 1. Exploded view of the CDI cell assembly. The inlet and outlet fittings, electrode contact screws and mounting bolts are omitted. The two aerogels are separated by a polymer mesh and are supported by titanium electrodes on the backside to decrease contact resistance. Rubber gasket is seated in a separate channel outside the test section.

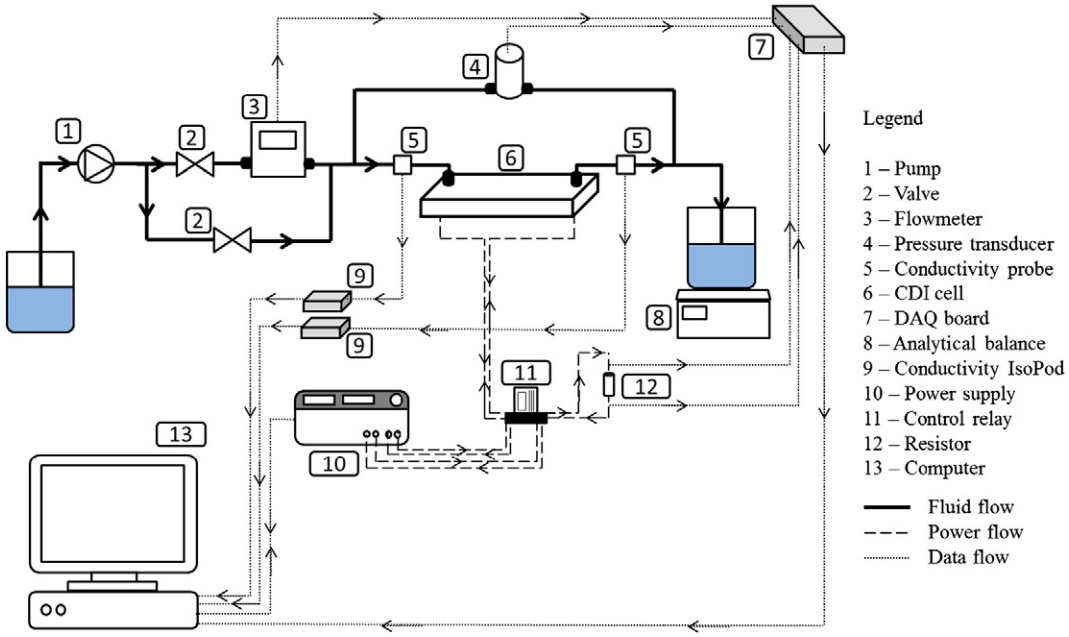

Fig. 2. Schematic overview of the experimental setup.

directly by an Omega Engineering FLR-1601A flow meter (±2% accuracy, for low flow rates) or by monitoring the rate of change of mass readings taken by A&D GH-252 analytical balance (±1.1% accuracy, for high flow rates) placed at the cell outlet. The pressure drop between the inlet and exit of the CDI cell is also monitored by an Omegadyne PX429 pressure transducer. The conductivity of inlet and outlet streams was measured with a pair of eDAQ Flow-Thru Conductivity ET908 sensors (±0.4% accuracy) connected to the computer via EP357 conductivity isoPods. The desalination or regeneration state for the CDI cell is determined by an NTE Electronics R14 DPDT relay, so that when the relay is powered, the anode and cathode of the CDI cell are connected to +1 V and ground poles of the power supply respectively, and when the relay is not powered, the anode and cathode of the CDI cell were connected through a 30.2 Ω resistor. The voltage drop across two ends of this resistor, the flowmeter reading and pressure transducer reading were collected by a National Instruments USB-6008 DAQ and sent to the computer via USB connection. The computer program was developed using National Instruments LabView software and it was used for monitoring and recording inlet and outlet conductivities, desalination and regeneration electric currents, flowmeter readings and pressure transducer readings. In addition, the durations for desalination and regeneration cycles, total number of cycles in a test, relay coil voltage and CDI cell voltage were all set through this program. The specifications for aforementioned instruments are presented in Table 1.

2.2. Experimental procedure

In the present work, two types of desalination experiments were performed: long-term steady tests, and alternating transient tests. A long-term steady desalination was first performed for every different salinity level and cell size. The data obtained from each steady test was then analyzed to estimate the three time instants later used to switch the system between desalination and regeneration during alternating transient tests. This procedure was first repeated for a single CDI cell system at inlet salinity levels of 0.5 $mg \cdot cm^{-3}$, 1.0 $mg \cdot cm^{-3}$ and 1.5 $mg \cdot cm^{-3}$ to observe the effects of salinity on CDI system performance. Then, tests at 1.0 $mg \cdot cm^{-3}$ were repeated for two and three cascaded CDI cells to observe the effects of size scaling on CDI system performance. Then the results from these transient tests were compared using the metrics introduced later in this section to evaluate the effects of timing, salinity and physical scale on CDI system performance.

The steady desalination tests are performed by applying a constant cell voltage of 1 V across the two electrodes of the CDI cell until the porous carbon aerogels are totally saturated. This condition is identified by comparing inlet and outlet conductivities, and thus concentrations. From a control volume perspective, whenever there is a net adsorption of ions within the CDI cell, the outlet concentration should be lower than inlet concentration. This means that the saturation occurs when the outlet concentration rises back up to the inlet concentration level, indicating no net adsorption.

Table 1
Instrument specifications.

Device		Range	Resolution	Accuracy
Agilent E3647A power supply	Voltage	0 to +35 V	<5 mV	±.05% + 5 mV
	Current	0 to 0.8 A	<1 mA	±.02% + 10 mA
Aqua Lifter AW-20 pump	Pressure	0 to ~7.5 kPa	–	–
	Flow rate	0 to 220 cm^3/min		
Omega Eng. FLR-1601A flowmeter		.01 to 0.5 sccm	.01 sccm	±2%
Omegadyne PX429 pressure transducer		0 to ~2.5 kPa	–	±.08%
eDAQ ET908 conductivity sensor		0 to 200 mS/m	–	±.4%

The transient desalination tests are performed by switching the CDI cell between desalination and regeneration at the time instants found by analyzing the steady test data. Approximately fifteen to thirty (depending on cycle duration) transient cycles were included in each transient test, to assure that repeatability among each cycle can be obtained and the initial transients of the cell do not affect the test results. The ionic adsorption, energy input and energy recovery were calculated for every cycle to be used in analysis.

A detailed description of the procedure for steady and transient test is presented by Clifton et al. [23].

2.3. Characteristic times

By running a steady test, three characteristic times were identified as having the ability to potentially optimize the operation of a transient system. These times correspond to the instants when: the output stream conductivity is minimum, t_1, the average ionic adsorption rate is maximum, t_2, and the amount of ions adsorbed per unit energy input into the system is maximum, t_3. Eqs. (1) to (3) detail the estimation of these three times.

$$t_1 = t[\min(\sigma)] \tag{1}$$

$$t_2 = t\left\{ \max\left[\frac{N_A}{F\cdot\left(\nu^{Cl^-}+\nu^{Na^+}\right)} \frac{(\sigma_0-\sigma)}{\int_0^t d\tau} \right] \right\} \tag{2}$$

$$t_3 = t\left\{ \max\left[\frac{N_A\cdot Q}{F\cdot\left(\nu^{Cl^-}+\nu^{Na^+}\right)} \frac{(\sigma_0-\sigma)}{\int_0^t I\cdot d\tau} \right] \right\} \tag{3}$$

Here σ and σ_0 (S m^{-1}) are the outlet and inlet solution conductivities respectively, N_A is Avogadro's number, Q (m$^3\cdot$s^{-1}) is the solution flow rate, F (C$\cdot$mol^{-1}) is the Faraday's constant, ν^{Cl-} and ν^{Na+} (m$^2\cdot$V$^{-1}\cdot$s^{-1}) are chloride and sodium ion mobilities respectively and I (A) is the electrical current that flows through the system during desalination.

The criteria and switching times presented above are illustrated in Fig. 3. In this figure, the outlet stream conductivity is normalized by its initial value, while the amount of ions adsorbed per unit energy input and the average adsorption rate are standardized by their respective maximum values. The actual times t_1, t_2, and t_3 obtained from these experiments are listed in Table 2. These times served to calibrate the switching times for the change from a desalination cycle to the regeneration cycle in a transient experiment.

Table 2
Summary of the desalination/regeneration cycle durations.

		CDI system size		
		1 cell	2 cells	3 cells
Concentration (mg/cm^3)	0.5	t_1 = 1080 s t_2 = 1656 s t_3 = 2204 s		
	1.0	t_1 = 860 s t_2 = 1361 s t_3 = 1913s	t_1 = 934 s t_2 = 2141 s t_3 = 3656 s	t_1 = 5002 s t_2 = 6676 s t_3 = 9679 s
	1.5	t_1 = 266 s t_2 = 492 s t_3 = 809 s		

Switching the CDI system from desalination to regeneration at the point of minimum outlet concentration, given as t_1 in Eq. (1), is an intuitive choice, as the minimum outlet concentration corresponds to maximum adsorption rate and reaching this point is usually desired. This is the simplest timing point, which will be compared to the optimized timing points given in Eqs. (2) and (3) to quantify possible performance improvements.

The second criterion can be used when the maximum ionic adsorption rate is desired from the CDI system. The adsorption rate of the CDI system is calculated as the product of flow rate and the concentration difference of inlet and outlet solutions, therefore the adsorption rate changes throughout the desalination process. Although maximum instantaneous adsorption rate corresponds to the instant when outlet conductivity is minimized, at time t_1, the maximum average adsorption rate throughout the desalination corresponds to time t_2, which is expected to be a better measure of overall desalination rate.

The final approach is to switch the system from desalination to regeneration at the instant adsorbed ions per input energy is maximized, which corresponds to time t_3. The main aim of this approach is operating the CDI system at the point of maximum "adsorption efficiency". This is related to the fact that after some point in desalination, the energy input-ion adsorption behavior of the system follows a diminishing returns behavior, meaning that after time t_3, continuing the desalination process is not energetically efficient. This effect can be seen when the time behavior of conductivity and input current are observed. The adsorption rate initially increases and then decreases back to zero with electrode saturation, while the input

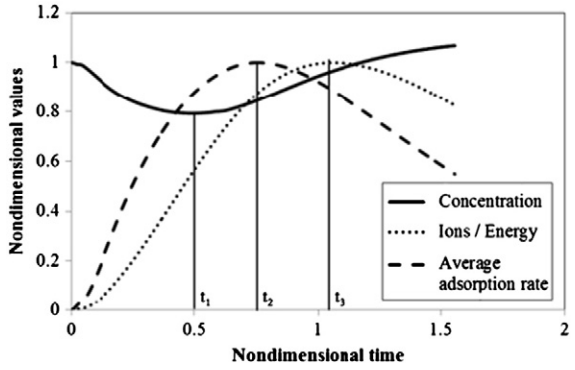

Fig. 3. Transient behavior of various nondimensionalized parameters during a steady test. The outlet concentration over time, ions per energy input, and average adsorption rate during desalination process.

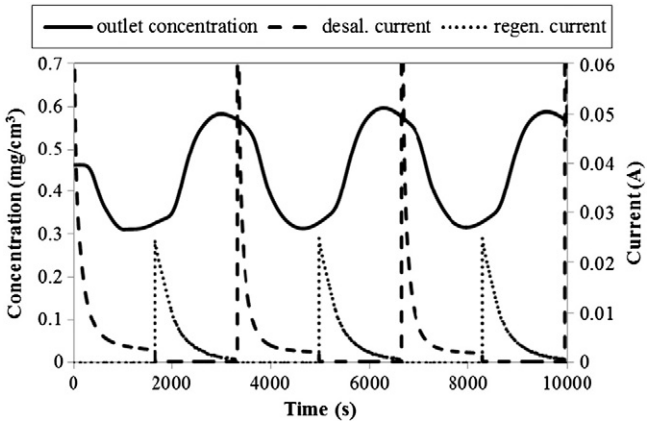

Fig. 4. Concentration and current behavior in a transient test. Current leakage is seen as non-zero desalination current towards the end of desalination. Oscillations in outlet conductivity have a delay due to the finite volume between CDI cell exit and conductivity probe.

power peaks at the beginning of desalination and decreases to a finite value as the electrodes are saturated. This is due to current leakage between the electrodes through the solution, shown in Fig. 4.

Before continuing, it must be noted that since the analysis to determine t_1, t_2, and t_3 was based on the desalination process, no specific criteria was considered to determine the elapsed time for the regeneration process. Therefore, for this paper, the regeneration and desalination times were set equal to each other for all the cases analyzed. In addition, flow rate was kept constant for every test, therefore the effect of flow rate on system performance is not considered.

2.4. Proposed evaluation criteria

Three criteria were used to evaluate the performance of a CDI system operating in alternating desalination–regeneration transient mode: energy recovery ratio, amount of salt adsorbed per unit volume of solution treated per unit energy, and thermodynamic efficiency.

2.4.1. Energy recovery ratio

This criterion relates the magnitude of the desalination energy input to the amount of energy obtained from the CDI cell during its regeneration. The energy delivered to the system during desalination, E_{in}, and recovered during the electrode regeneration, E_{regen}, was estimated as:

$$E_{in} = \int_0^t V \cdot I \cdot d\tau, \tag{4}$$

$$E_{regen} = \int_0^t I^2 \cdot R \cdot d\tau, \tag{5}$$

where V is the constant electric potential applied to the desalination cell in volts (1.0 V for this paper), and R is the electric resistance connected to the desalination cell during its regeneration (30.2 Ω). The energy recovery percentage is calculated from the ratio of these values.

One important point to note is that this metric does not take the adsorption performance into account, which indicates that it is a measure of energy consumption, not energy efficiency. Therefore, systems with lower energy recovery ratio might actually have higher energy efficiency, which is the reason for introducing the following two metrics.

2.4.2. Amount of salt adsorbed per unit volume of solution treated per unit energy

This parameter was estimated as:

$$\frac{\text{Adsorbed ions}}{\text{Energy} \cdot \text{Volume}} = \frac{\dfrac{N_A \cdot Q}{F \cdot \left(\nu^{Cl^-} + \nu^{Na^+}\right)}(\sigma_0 - \sigma)}{\displaystyle\int_0^t I \cdot d\tau \int_0^t Q \cdot d\tau}. \tag{6}$$

This standard provides a baseline comparison across the variety of different system configurations and is arguably the best method of extrapolating system performance on a large scale. While producing a large amount of ionic concentration change per unit of solution volume is desirable, it is also important that the energy cost of this change should not be prohibitively large. Both of these effects are considered in this performance metric. However, according to this metric, desalinating a certain amount of ions at different salinity levels results in the same performance, provided that the energy consumption and volume of treated solution are equal, which should not be the case. This point is addressed by introducing the thermodynamic efficiency metric, presented below.

2.4.3. Thermodynamic efficiency

Thermodynamic efficiency, η_{th}, in the scope of this study is the ratio of reversible work, W_{rev}, needed to separate a saline solution into a dilute product and a concentrated brine stream, to the net energy requirement, W_{in}, of the experimental capacitive deionization system:

$$\eta_{th} = \frac{W_{rev}}{W_{in}}. \tag{7}$$

The estimation of the reversible work based on the second law of thermodynamics is parallel to the energetic analysis presented by Spiegler and El-Sayed for ideal liquid solutions and salt-free product water in five desalination technologies other than capacitive deionization [24]. The present paper, however, assesses the desalination process as a separation of the inlet solution into lower salinity product and concentrated brine solutions, which has been demonstrated for multiple effects evaporation (MEE) desalination [25].

For a constant temperature and pressure desalination process, the reversible work equals the change in Gibbs free energy, ΔG, due to concentration difference. Assuming an ideal solution, the chemical activities in the inlet and outlet streams would equal their molar concentrations. Therefore, the variation in free Gibbs energy can be estimated as [26]:

$$\Delta G = \left(\sum_{out} n_i \cdot RT \ln(x_i)\right) - n_{in} \cdot RT \ln(x_{in}) \tag{8}$$

where n (mol) is the amount of solutes passing through the CDI cell, R is the ideal gas constant (8.31416 J·mol·K^{-1}), T (K) is the solution temperature, x is the average molar fraction of the solution (averaged over time in this paper), and the subscripts *in* and *out* denote the inlet stream and outlet streams (either product or brine) respectively.

To validate the ideal solution assumption, the mean ionic activity coefficient, $\gamma_{\pm}$, for a 0.5 mg·cm^{-3} NaCl solution at 298 K was calculated from the Debye–Huckel theory of electrolytes [27] as 0.96, which is approximately equal to 1 in the scope of this study. Therefore, it can be said that Eq. (8) is valid for this case. A drawback of using this metric is that it is an indication of desalination efficiency, not desalination rate. Since the desalination rate is addressed by the previous metric, it is expected that these two metrics should be used together to have a better understanding of system performance.

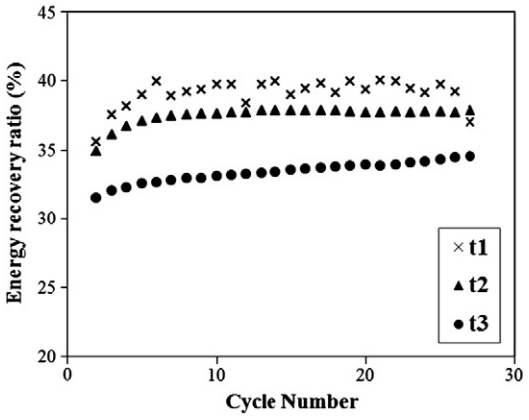

Fig. 5. Energy recovery ratio during regeneration of the capacitive deionization system. Results indicate an inverse proportionality between energy recovery ratio and desalination–regeneration duration. Error bars not shown due to negligible electrical measurement errors.

3. Results and discussion

Performance of a CDI system operating at different desalination and regeneration durations is analyzed for various salinity levels and various CDI system sizes. The results of these analyses are presented in three sections to observe the effects of timing, salinity and scale on CDI system performance independently.

3.1. Effect of timing on system performance

Three different timing approaches are compared for a single cell CDI system operating at 1.0 $mg \cdot cm^{-3}$ inlet salinity level and 0.5 $cm^3 \cdot min^{-1}$ solution flow rate and the results are presented below.

3.1.1. Energy recovery ratio

The energy recovery results, presented in Fig. 5, reach 40% for a simple experimental CDI cell, which seems promising for the production of an industrial capacitive desalination plant with even greater efficiency. For every test, it is seen that the energy recovery increases during the first cycles and stabilizes at a certain point, after the first 15 cycles for this case.

Calibrating the system at the minimum outlet concentration, t_1, yields the best energy recovery results, which points to the possibility of t_1 being the most energy efficient timing. Timing the desalination system with respect to maximum energy efficiency, t_3, results in the worst energy recovery results, whereas timing with respect to maximum average adsorption rate, t_2, results in an intermediate energy recovery ratio. Comparing these three cases, it is seen that energy recovery ratio is inversely proportional to cycle duration. This is predicted to be due to the leakage current between electrodes during desalination, whose effect becomes more pronounced as the desalination duration increases. This means that desalination–regeneration duration approaching infinity would result in an energy recovery ratio approaching zero.

3.1.2. Amount of salt adsorbed per unit volume of solution treated per unit energy

As seen in Fig. 6, system calibration with respect to t_2 results in the highest amount of ions adsorbed per volume per energy for the first 15 cycles. After that, it stabilizes at almost the same performance level as system calibrated with respect to t_3, albeit still higher. Considering that CDI systems are supposed to operate for many consecutive cycles, it can be said that t_2 results in a slightly higher performance than t_3 according to this metric. System calibration with the timing t_1 results in the worst performance, which is an indication that energy recovery results by themselves are not a good indication of overall system performance, which includes adsorption performance.

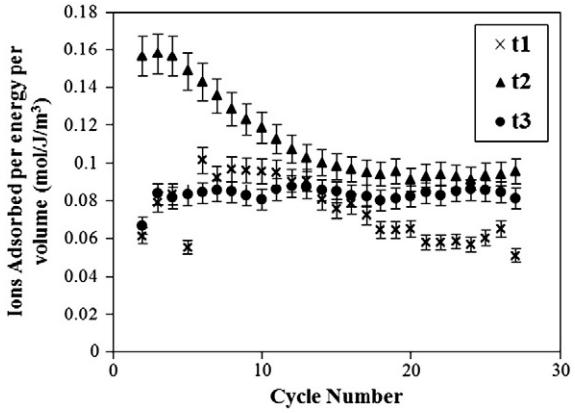

Fig. 6. Number of ions adsorbed during desalination per unit energy input and unit volume per cycle. Comparison between the transient tests operating at three different cycle durations shows t_2 to have the highest performance according to this metric. The errors are due to uncertainties in flow rate and conductivity measurements.

An interesting point in comparison of the times is seen when adsorbed ions per input energy and adsorbed ions per volume of treated solution are considered separately. It was seen that system calibration with respect to time t_3 results in the highest value of adsorbed ions per input energy, calculated as: $(5.35 \pm 1.11) \cdot 10^{-7}$, $(1.21 \pm 0.25) \cdot 10^{-6}$ and $(1.38 \pm 0.06) \cdot 10^{-6}$ $mol \cdot J^{-1}$ for t_1, t_2 and t_3 respectively. On the other hand, system calibration with respect to t_2 results in the highest value of adsorbed ions per volume of solution treated, calculated as: (0.71 ± 0.16), (1.26 ± 0.30) and (0.97 ± 0.04) $mols \cdot m^{-3}$ for t_1, t_2 and t_3 respectively. This indicates that the operating conditions of the CDI system can be chosen according to specific needs. If the desalination rate is the crucial factor, one should choose to operate the system close to t_2, with shorter desalination and regeneration cycles. On the other hand, if energy efficiency is the most important factor, one should choose to operate close to t_3, with longer desalination and regeneration cycles.

3.1.3. Thermodynamic efficiency

The thermodynamic efficiency results are presented in Table 3 for each desalination/regeneration cycle duration. It is seen that timing t_3 results in the highest thermodynamic efficiency, with t_2 showing somewhat inferior performance. Timing with respect to minimum outlet conductivity, however, results in a thermodynamic efficiency value 0.19%, which significantly less than the other two timing methods.

The results of thermodynamic efficiency calculations are within expectations. Timing t_3 is based on maximizing the energy efficiency of CDI system and therefore results in the highest thermodynamic efficiency. Timing t_2 represents a calibration for maximum adsorption rate; therefore some concession in energy efficiency has to be made, which is seen in the decrease of thermodynamic efficiency from 0.38% to 0.35%.

3.2. Effect of solution concentration on system performance

The testing procedure, including timing with respect to three criteria and performance evaluation based on transient tests, was performed for a single CDI cell, constant 0.5 $cm^3 \cdot min^{-1}$ solution flow rate and three different inlet solution salinity levels: 0.5 $mg \cdot cm^{-3}$, 1.0 $mg \cdot cm^{-3}$ and 1.5 $mg \cdot cm^{-3}$.

3.2.1. Energy recovery ratio

The results, tabulated in Table 4, indicate that the energy recovery ratio of the system increases with the inlet solution salinity. This can be interpreted as the effect of remnant ions (from previous cycles) inside the porous electrodes on desalination and regeneration, which is more pronounced at higher salinity conditions.

If the electrodes are not totally clean at the beginning of desalination, the number of ions adsorbed during the desalination cycle and also the input energy during desalination decreases. However, the total number of ions stored in the electrodes at the end of desalination is still more than it would be for a desalination cycle started with a completely clean electrode. This causes the regeneration current to increase, therefore increasing the energy recovery ratio. However, as will be discussed later, the decrease in adsorption performance is more than the increase

Table 3
Thermodynamic efficiency results.

Test	Reversible energy input (J)	Actual energy input (J)	Thermodynamic efficiency
t_1	0.35	185.2	0.19%
t_2	0.82	232.2	0.35%
t_3	0.91	236.9	0.38%

Table 4
Summary of performance evaluation at different concentrations. Points of maxima are indicated in bold.

Concentration (mg/cm^3)		Energy recovery (%)	Ions/(energy · volume) (mol/J/m^3)	Thermodynamic efficiency (%)
0.5	t_1	28.5 ± 1.3	0.028 ± 0.003	0.17 ± 0.02
	t_2	**29.1 ± 0.2**	**0.036 ± 0.003**	0.47 ± 0.05
	t_3	28.2 ± 1.0	0.032 ± 0.004	**0.68 ± 0.07**
1.0	t_1	**39.1 ± 1.0**	0.075 ± 0.015	0.19 ± 0.02
	t_2	37.5 ± 0.6	**0.092 ± 0.022**	0.35 ± 0.04
	t_3	33.4 ± 0.7	0.086 ± 0.004	**0.38 ± 0.04**
1.5	t_1	**63.1 ± 1.0**	0.013 ± 0.004	0.03 ± 0.01
	t_2	52.9 ± 0.6	0.036 ± 0.012	0.07 ± 0.01
	t_3	46.3 ± 0.5	**0.080 ± 0.015**	**0.1 ± 0.01**

in energy recovery ratio, meaning that an increase in energy recovery ratio by itself does not mean that a system is more efficient.

One might expect to see a decrease in energy recovery ratio as the salinity level increases, because the resistivity of solution would decrease as the salinity increases, causing an increase in the leakage current, mentioned previously. When the desalination current behaviors are compared for individual cycles at different salinity levels, it is seen that the leakage current is indeed greater for higher salinity solutions, but the effect of remnant ions have a greater impact on energy recovery ratio.

3.2.2. Amount of salt adsorbed per unit volume of solution treated per unit energy

According to Table 4, it is obvious that there is not a simple trend between this performance metric and solution salinity level.

When the system performance for 0.5 mg·cm^{-3} solution and 1.0 mg·cm^{-3} solution is observed, it is seen that there is a significant increase in performance as the salinity level is doubled. It is seen that the energy consumption at these conditions was quite close, whereas the number of ions adsorbed was higher and desalination/regeneration cycles were shorter for 1.0 mg·cm^{-3} solution. Therefore, it can be said that the performance increases with salinity up to a certain level, due to more effective adsorption at higher salinity levels.

If the same performance comparison is made between 1.0 mg·cm^{-3} and 1.5 mg·cm^{-3} solutions, the opposite effect is observed. The performance of the system decreases drastically as the salinity is increased from 1.0 mg·cm^{-3} to 1.5 mg·cm^{-3} and only the timing t_3 results in acceptable performance at 1.5 mg·cm^{-3}, while still inferior to 1.0 mg·cm^{-3} results. Therefore, it can be deducted that a CDI system of this size is beyond its optimal operation range at such high salinity levels.

The outlet conductivity and desalination/regeneration current data were investigated to find the source of the system inefficiency at high salinity, and it was seen that the decrease in conductivity was significantly lower than the steady test conditions during desalination of 1.5 mg·cm^{-3} solutions. This points to the effect of remnant ions mentioned before, and it is clearly seen at this conductivity level that remnant ions from previous cycles are a significant cause of performance deterioration. This effect is less pronounced when the system is operated at t_3, the longest time, which is thought to be due to more efficient regeneration of the system.

3.2.3. Thermodynamic efficiency

It is clearly seen that the thermodynamic efficiency of the system decreases as inlet solution concentration increases. The first reason for this behavior is that the increase in solution salinity results in a decrease in solution resistivity, and subsequently an increase in leakage current. This increases the energy consumption of the system, resulting in lower thermodynamic efficiency.

One other effect that causes such a decrease in thermodynamic efficiency at higher salinity levels is the outlet conductivity behavior. The outlet conductivity shows a periodic oscillation behavior around the inlet conductivity level, decreasing during desalination and increasing during regeneration, as seen in Fig. 4. One of the factors that affect the magnitude of these oscillations is the limited electrode surface area and ionic capacity. At low concentrations, the outlet conductivity is significantly decreased during desalination cycles and significantly increased during regeneration, whereas these concentration oscillations get smaller and smaller compared to inlet concentration as it is increased. This has two effects: firstly, the lower magnitude of oscillations decreases the reversible work input necessary and secondly, even if the oscillation magnitudes were the same, reversible work to cause the same amount of concentration oscillation is lower at higher salinity levels, due to the logarithmic behavior of Gibbs free energy function. These two factors mean that the thermodynamic efficiency of a CDI system decreases with increasing salinity level.

3.3. Effect of CDI system size on system performance

Three CDI cells of the same specifications have been manufactured and cascaded as needed to measure the performance of CDI system operating at constant 0.5 cm^3·min^{-1} solution flow rate and 1.0 mg·cm^{-3} inlet salinity level, for different sizes, using one, two or three cells.

3.3.1. Energy recovery ratio

As seen in Table 5, the energy recovery results do not follow a trend with CDI system size. The highest energy recovery values are obtained for the 2 cell system, followed by 1 cell system and 3 cell

Table 5
Summary of performance evaluation at different CDI system sizes. Points of maxima are indicated in bold.

System size (number of cells)		Energy recovery (%)	Ions/(energy · volume) (mol/J/m^3)	Thermodynamic efficiency (%)
1	t_1	**39.1 ± 1.0**	0.075 ± 0.015	0.19 ± 0.02
	t_2	37.5 ± 0.6	**0.092 ± 0.022**	0.35 ± 0.04
	t_3	33.4 ± 0.7	0.086 ± 0.004	**0.38 ± 0.04**
2	t_1	**48.1 ± 2.5**	0.025 ± 0.009	0.14 ± 0.01
	t_2	41.1 ± 0.7	0.049 ± 0.003	0.24 ± 0.03
	t_3	37.2 ± 1.0	**0.059 ± 0.011**	**0.49 ± 0.05**
3	t_1	**36.6 ± 1.7**	0.028 ± 0.007	0.28 ± 0.03
	t_2	32.2 ± 1.3	**0.037 ± 0.004**	0.58 ± 0.06
	t_3	29.4 ± 1.8	0.033 ± 0.006	**1.16 ± 0.13**

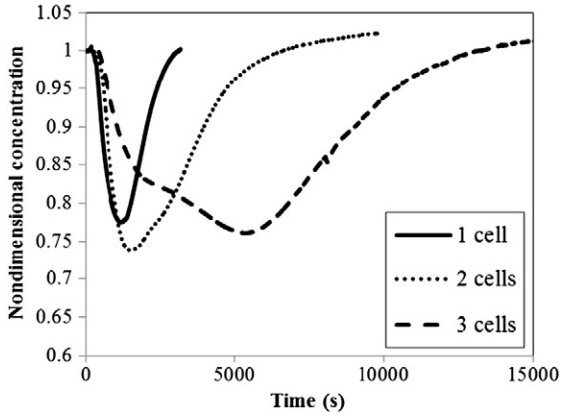

Fig. 7. Outlet concentration in steady tests for different CDI system sizes. It is seen that the adsorption capacity increases with system size, but the transient behavior also changes. This is thought to be due to connections (tubing) between CDI cells.

system in this order. This leads to the conclusion that energy recovery ratio is not directly correlated to CDI system size.

The difference in energy recovery ratios at different CDI system sizes leads to the suspicion that CDI cell assemblies were not up to the same specifications for different tests. However, the CDI cells were disassembled before starting experimentation at each CDI system size, were checked for any corrosion, leakage or fouling and were reassembled using new carbon aerogels of the same size. In addition, contact resistances at the terminals were checked before each test to have a consistent power supply to the system. Therefore, it is thought that the reason to have such a behavior of energy recovery is not experimental inconsistencies, but the change in the system transients at different CDI system sizes, which are seen to be changing with system size in Fig. 7.

One important point to note is that the inverse proportionality between cycle duration and energy recovery is also valid for all three different sized systems. This is in acceptance with the findings in previous sections.

3.3.2. Amount of salt adsorbed per unit volume of solution treated per unit energy

The test results, seen in Table 5, indicate that this metric is inversely proportional to the CDI system size. This metric takes both adsorption rate and energy efficiency into account, so the results can be analyzed by considering these effects separately.

When the ionic adsorption performance is compared between 1, 2 and 3 cell systems, it is seen that the amount of ions adsorbed at each cycle is directly proportional to CDI system size, as expected. Using timing t_3 as reference condition, the average amount of ions adsorbed in one cycle is $(1.55 \pm 0.07) \cdot 10^{-5}$, $(3.95 \pm 0.8) \cdot 10^{-5}$ and $(12.0 \pm 2.2) \cdot 10^{-5}$ mol for 1, 2 and 3 cell systems respectively. This increase is associated with the increased cell size and increased cycle durations due to slower saturation of bigger cells. In fact, one can compare the amount of ions adsorbed per volume of solution treated (indicative of adsorption rate) for three cases and see that it is (0.97 ± 0.04), (1.30 ± 0.27) and (1.50 ± 0.28) mols$\cdot$m^{-3} for 1, 2 and 3 cell systems respectively. This shows that there is an increase in average adsorption rate as the CDI system size increases, due to lower saturation effects.

The average energy consumption per desalination cycle is given as (11.2 ± 0.3), (21.7 ± 0.7) and (46.3 ± 2.3) J for 1, 2 and 3 cell systems respectively. This indicates an increase in energy consumption with increased system size, which is an expected result of parallel electrical connection of CDI cells.

Combining the two findings above, it is seen that increasing CDI system size results in higher amount of adsorbed ions and higher adsorption rate, but these advantages come at the cost of increased energy consumption. Since the increase in adsorption rate is not as drastic as the energy consumption, increasing CDI system size results in decreased amount of ions per energy input per volume of solution treated. Results of analysis indicate that scaling up is an obvious solution for increasing system capacity in terms of adsorption rate, but it is not useful for increasing performance with respect to this metric. This emphasizes the importance of system design and optimization at larger scales.

3.3.3. Thermodynamic efficiency

Results presented in Table 5 indicate that thermodynamic efficiency is directly proportional to system size. In addition, it is seen that timing t_3 results in the highest thermodynamic efficiency values for each CDI system size, which is in acceptance with the findings presented in Section 3.1.

The reasoning behind increasing thermodynamic efficiency with CDI system size can be better understood when the transient outlet conductivity behavior of the system is observed. As mentioned in Section 3.2.3, the outlet conductivity shows an oscillating behavior around inlet conductivity, decreasing during desalination and increasing during regeneration. The magnitudes of these oscillations were seen to be increasing with increasing CDI system size. This is an expected result, due to higher ionic capacity of the larger system and longer cycle durations. The increase in magnitude of oscillation of outlet conductivity means that not only the amount of adsorbed ions are increasing, but also the reversible energy required per adsorbed ions is increasing too. This is due to the logarithmic behavior of Gibbs free energy function, as mentioned before. It should be noted that this effect is not included in the calculation of number of ions per input energy per volume of solution treated, therefore the CDI system size dependence of these two metrics is opposite.

The results presented in Table 5 seem promising, in the sense that thermodynamic efficiency of the CDI system benefits from upscaling, which is necessary for practical applications.

4. Conclusions

This paper presents a novel methodology to determine the most favorable operational conditions for a capacitive deionization cell functioning at alternating transient desalination–regeneration processes. Also, three evaluation criteria based on the energetic performance of the system were proposed. These metrics were then used to evaluate the effects of CDI system size and inlet solution concentration on the overall system performance.

The results presented in this paper suggest that switching the CDI system from desalination to regeneration and vice versa to maximize the amount of ions adsorbed per unit energy (t_3) maximizes the thermodynamic efficiency of the system. On the other hand, timing the system to maximize the average adsorption rate during desalination (t_2) usually results in highest number of ions adsorbed per input energy per volume of solution treated. These two findings indicate that there exists two optimal operational points for a CDI system: maximum efficiency and maximum adsorption rate. One can choose to operate the system at either of these two points or somewhere in between, depending on the critical requirements, and the results indicate a trade-off between thermodynamic efficiency and adsorption rate. It was also seen that timing the system according to maxima and minima of outlet concentration might be the simplest solution, but it results in the lowest system performance according to all the metrics, except energy recovery ratio, which was shown to be insufficient by itself to measure the energetic performance.

Experimental results indicate that energy recovery ratio is directly proportional to inlet solution concentration, due to the effect of incomplete regeneration and remnant ions from previous cycles. On the other hand, thermodynamic efficiency is inversely proportional to inlet solution concentration, which points to deteriorating system performance at higher salinity levels. Therefore, it can be said that there exist a higher

limit of solution concentration which can be economically and practically processed by a CDI system of certain size.

The results also indicate that increasing system size provides an increase in thermodynamic efficiency. This was seen to be due to the higher system capacity enabling a more significant drop in outlet conductivity during desalination. This is a promising result which should provide motivation to build larger scale CDI systems and to make commercial CDI systems a reality.

Acknowledgments

The authors would like to thank Rebecca Clifton, Brian Carroll, and Collier Miers for their help in the fabrication and programming of the experimental set-up. This research was funded by The University of Texas start-up funds and The University of Texas System STARS.

References

[1] U. S. C. Bureau, U.S. & World Population Clocks. Available: http://www.census.gov/main/www/popclock.htmlMay 15 2012.
[2] M.A. Anderson, A.L. Cudero, J. Palma, Capacitive deionization as an electrochemical means of saving energy and delivering clean water. Comparison to present desalination practices: will it compete? Electrochim. Acta 55 (2010) 3845–3856.
[3] T.J. Welgemoed, C.F. Schutte, Capacitive deionization technology (TM): an alternative desalination solution, Desalination 183 (2005) 327–340.
[4] Coping with Water Scarcity: Challenge of the 21st Century. Available: http://www.fao.org/nr/water/docs/escarcity.pdf2007.
[5] J. McGlade, B. Werner, M. Young, M. Matlock, D. Jefferies, G. Sonnemann, M. Aldaya, S. Pfister, M. Berger, C. Farell, K. Hyde, M. Wackernagel, A. Hoekstra, R. Mathews, J. Liu, E. Ercin, J.L. Weber, A. Alfieri, R. Martinez-Lagunes, B. Edens, P. Schulte, S. von Wirén-Lehr, D. Gee, Measuring Water Use in a Green Economy, UNEP, 2012.
[6] I.A. Shiklomanov, World Water Resources: Modern Assessment and Outlook for the 21st Century, UNESCO — Federal Service of Russia for Hydrometerology & Environment Monitoring, 1999.
[7] C. o. A. D. Technology and N. R. Council, Desalination: A National Perspective, The National Academies Press, 2008.
[8] M. Al-Shammiri, M. Safar, Multi-effect distillation plants: state of the art, Desalination 126 (1999) 45–59.
[9] Y.-J. Kim, J.-H. Choi, Enhanced desalination efficiency in capacitive deionization with an ion-selective membrane, Sep. Purif. Technol. 71 (2010) 70–75.
[10] D. Vial, G. Doussau, The use of microfiltration membranes for seawater pretreatment prior to reverse osmosis membranes, Desalination 153 (2003) 141–147.
[11] J. Newman, Engineering design of electrochemical systems, Ind. Eng. Chem. 60 (04/01/1968) 12–27.
[12] A.M. Johnson, J. Newman, Desalting by means of porous carbon electrodes, J. Electrochem. Soc. 118 (1971) 510–517.
[13] R.W. Pekala, J.C. Farmer, C.T. Alviso, T.D. Tran, S.T. Mayer, J.M. Miller, B. Dunn, Carbon aerogels for electrochemical applications, J. Non-Cryst. Solids 225 (1998) 74–80.
[14] J.-A. Lim, N.-S. Park, J.-S. Park, J.-H. Choi, Fabrication and characterization of a porous carbon electrode for desalination of brackish water, Desalination 238 (2009) 37–42.
[15] K.-K. Park, J.-B. Lee, P.-Y. Park, S.-W. Yoon, J.-S. Moon, H.-M. Eum, C.-W. Lee, Development of a carbon sheet electrode for electrosorption desalination, Desalination 206 (2007) 86–91.
[16] K. Dermentzis, K. Ouzounis, Continuous capacitive deionization–electrodialysis reversal through electrostatic shielding for desalination and deionization of water, Electrochim. Acta 53 (2008) 7123–7130.
[17] I. Villar, S. Roldan, V. Ruiz, M. Granda, C. Blanco, R. Menéndez, R. Santamaría, Capacitive deionization of NaCl solutions with modified activated carbon electrodes†, Energy Fuel 24 (06/17/2010) 3329–3333.
[18] M. Mossad, L. Zou, A study of the capacitive deionisation performance under various operational conditions, J. Hazard. Mater. 213–214 (2012) 491–497.
[19] Y. Bouhadana, E. Avraham, M. Noked, M. Ben-Tzion, A. Soffer, D. Aurbach, Capacitive deionization of NaCl solutions at non-steady-state conditions: inversion functionality of the carbon electrodes, J. Phys. Chem. C 115 (08/25/2011) 16567–16573.
[20] P. Xu, J.E. Drewes, D. Heil, G. Wang, Treatment of brackish produced water using carbon aerogel-based capacitive deionization technology, Water Res. 42 (2008) 2605–2617.
[21] O.N. Demirer, R.L. Clifton, C.A. Rios Perez, R. Naylor, C. Hidrovo, Characterization of Ion Transport and -Sorption in a Carbon Based Porous Electrode for Desalination Purposes, ASME J. Fluids Eng. (accepted for publication) (Article DOI Number: 10.1115/1.4023294).
[22] Y. Bouhadana, M. Ben-Tzion, A. Soffer, D. Aurbach, A control system for operating and investigating reactors: the demonstration of parasitic reactions in the water desalination by capacitive de-ionization, Desalination 268 (2011) 253–261.
[23] R.L. Clifton, C.A. Rios Perez, R. Naylor, C. Hidrovo, Characterization of ion transport and -sorption in a carbon based porous electrode for desalination purposes, 10th International Conference on Nanochannels, Microchannels, and Minichannels, Rio Grande, Puerto Rico, 2012, p. 9.
[24] K.S. Spiegler, Y.M. El-Sayed, The energetics of desalination processes, Desalination 134 (2001) 109–128.
[25] A. Piacentino, E. Cardona, Advanced energetics of a Multiple-Effects-Evaporation (MEE) desalination plant. Part II: potential of the cost formation process and prospects for energy saving by process integration, Desalination 259 (9/15/2010) 44–52.
[26] A. Bejan, Advanced Engineering Thermodynamics, 3rd ed. Wiley, John & Sons, Inc., 2006
[27] P. Atkins, J. de Paula, Atkin's Physical Chemistry, Eighth ed. Freeman, W. H. & Company, 2006.